Comparative studies of Rhodamine B decolorization in the combined process Na$_2$S$_2$O$_8$/visible light/ultrasound

Piotr Zawadzki

Laboratory of Water and Sewage Technologies, Department of Water Protection, Central Mining Institute,
Plac Gwarków 1, 40-166 Katowice, Poland, Tel. 0048 32 259-28-01; email: pzawadzki@gig.eu

ABSTRACT

In this study, the possibility of rhodamine B (RhB) decomposition in the presence of ultrasound (US) and sodium persulfate (Na$_2$S$_2$O$_8$) activated by visible light (Vis) was investigated. A combination of these processes (Na$_2$S$_2$O$_8$/Vis/US) were examined. As a part of this study, the optimal dose of Na$_2$S$_2$O$_8$, glucose dose, reaction time, and RhB concentration were selected. In addition, radical scavenger test was conducted. Under optimal conditions (RhB concentration = 10.0 mg dm^{-3}; pH = 6.0; reaction time: 60.0 min; Na$_2$S$_2$O$_8$ dose = 20.0 mM; glucose dose = 200.0 mM; US power: 60 W; US frequency: 40 kHz; temperature: 295 K), RhB decomposition in the Na$_2$S$_2$O$_8$/Vis/US process was set to 85%. Under the same conditions, the RhB decomposition in the US, Na$_2$S$_2$O$_8$, Na$_2$S$_2$O$_8$/Vis and Na$_2$S$_2$O$_8$/US processes was 17%, 29%, 49% and 67%, respectively. The determined parameters of the pseudo-first-order reaction showed the advantage of the dynamics of the Na$_2$S$_2$O$_8$/Vis/US process over the US, Na$_2$S$_2$O$_8$, Na$_2$S$_2$O$_8$/Vis and Na$_2$S$_2$O$_8$/US processes. The mathematically calculated half-life (t/2) for the combined process was 2.1 min, while half-life values for the US, Na$_2$S$_2$O$_8$, Na$_2$S$_2$O$_8$/Vis and Na$_2$S$_2$O$_8$/US processes are 25.5, 15.9, 7.8 and 4.6 min, respectively. Hydroxyl radicals were mainly responsible for the decolorization of rhodamine B. The conducted studies showed that the activation of sodium persulfate in the combined process of sodium persulfate-visible light-ultrasound is an interesting alternative for the purification of solutions containing rhodamine B with variable dye concentrations (up to 20 mg dm^{-3}).

Keywords: Rhodamine B; Advanced oxidation process; Sodium persulfate; Visible light; Ultrasound

1. Introduction

In the presence of the deepening global water crisis, the world may experience a 40% reduction in water availability by 2030. It is predicted that half of the world's population will be at risk of water scarcity by 2050 [1]. The presence of organic and inorganic compounds disturbing the functioning of living organisms in water ecosystems is of great concern these days. These substances are classified as micropollutants, and their presence in aquatic ecosystems is documented. Micropollutants are usually defined as compounds occurring in concentrations of ng/dm^3 or mg/dm^3. Micropollutants are characterized by two toxic effects namely: (1) effects that appear after a short time of exposure and (2) effects that appear after a long time (long-term health effects). Micropollutants can generally be divided into organic and inorganic substances. The organic group of micropollutants is very extensive and may include endocrine active compounds, disinfection by-products, polychlorinated biphenyls, pesticides, dyes, surfactants and

polycyclic aromatic hydrocarbons [2–5]. Among the compounds belonging to the group of micropollutants, there are rhodamines – organic chemical compounds from the group of triphenylmethyl xanthene dyes. Rhodamine B (RhB) is a compound which belongs to this group.

Rhodamine B is used as a dye in numerous industries, such as chemical, textile, paper or dyeing. It is a fluorescent dye, which is also used in biological research on animals due to its easy accumulation, for example, in animal hair and teeth. RhB is toxic to humans and animals. Symptoms of the negative influence of this chemical compound are skin, eyes and respiratory system irritation. It also displays mutagenic and carcinogenic potential. This dye has a high affinity for proteins involved in basic cell metabolism [6,7].

The development of industry leads to the fact that rhodamine B is one of the main components identified in the industrial wastewater of dyeing and textile. The use of conventional purification processes such as activated carbon, coagulation, filtration, activated sludge does not bring satisfactory results due to high concentration of dyes, low biodegradability and higher stability of newly synthesized dyes [8]. For this reason, it is justified to search for new solutions in the field of water and wastewater treatment.

Advanced oxidation processes (AOPs) have gained great interest in the recent years. AOPs are listed as one of the best available techniques for colored wastewater treatment [9]. A common feature of AOPs is the oxidation of organic compounds by generating hydroxyl radicals $OH^{\bullet}$ ($E^0 = 2.80$ V). Scientific data show that a lot of work is devoted to the use of sulfate radicals $SO_4^{\bullet-}$ ($E^0 = 2.50$–3.10 V) for the decomposition of organic pollutants [10,11]. The generation of sulfate radicals occurs through the activation of persulfate ions ($S_2O_8^{2-}$) by means of UV radiation, heat, ionizing radiation, high pH and transition metal ions [12–16]. Activation with transition metal ions at low oxidation levels such as Fe^{2+}, Ni^{2+}, Co^{2+} and Ag^+ is most commonly used. Persulfates react with the transition metal electron donor to form a single sulfate radical (Eq. (1)) [17].

$$S_2O_8^{2-} + e^- \rightarrow SO_4^{2-} + SO_4^{\bullet-} \tag{1}$$

The high cost of conventional activation methods indicates that new methods for the generation of sulfate radicals are gaining interest. New methods of activation, for example, ultrasound, ozone or carbon nanotubes are studied [18,19]. However, there are few studies on the activation of persulfates with visible light [20,21]. This is due to the very poor quantum efficiency of sulfate radicals at the wavelength of $\lambda > 400$ nm [22].

Unconventional methods of activation should be equally efficient and cost-effective compared with conventional methods. Materials that allow the activation of persulfates (PDS) under the influence of visible light may be, for example, acids and sugars [23]. Sugar prices may be even twice lower compared with $FeSO_4 \cdot 7H_2O$, a compound commonly used to activate persulfates. Moreover, sugars are ingredients present in wastewater. Thus, a fully-recognized wastewater composition will minimize the amount of this reagent. In addition, the dose of sugars used to activate PDS is too low to be toxic to living organisms.

The use of ultrasound is a hybrid method of activation. During the ultrasound process, the cavitation bubbles break down, which locally causes the formation of high temperatures and pressure. The combination of these factors generates hydroxyl ($OH^{\bullet}$), superoxide ($O_2^{\bullet-}$) and H_2O_2 [24,25] radicals. Ultrasonic technology is a safe and efficient method for potential use in water and wastewater treatment. Activation of PDS with ultrasound is characterized by higher efficiency compared with, for example, the $H_2O_2/$US system [26,27].

The aim of this study is to assess the efficiency of rhodamine B degradation in the AOP carried out in the presence of sodium persulfate activated by visible light and ultrasound. The optimum doses of PDS and glucose have been carried out. The effect of initial RhB concentration on the final degree of dye decolorization was investigated.

2. Materials and methods

2.1. Model solution

Model solutions were prepared on the basis of deionized water with the addition of rhodamine B (RhB) standard. The physical and chemical characteristics of RhB are presented in Table 1. Dye with a purity of ≥95.0% was obtained from Sigma-Aldrich (Poznań, Poland). The pH of the model solution before and after the addition of the dye solution was pH = 6.0. Any deviations from this value were corrected with 0.1 mol dm⁻³ HCl or 0.1 mol dm⁻³ NaOH from Sigma-Aldrich. The pH of the model solution was monitored using a CPC-511 pH meter from Elmetron (Zabrze, Poland). Other analytical grade reagents used

Table 1
Physicochemical characteristics of rhodamine B [28]

Chemical structure	Physicochemical properties	
	Chemical formula	$C_{28}H_{31}ClN_2O_3$
	Molecular weight (g mol⁻¹)	479.01
	Nr CAS	81–88–9
	Water solubility at 20°C (g dm⁻³)	15.0
	Dissociation constant (pKa)	3.7
	logK_{OW}	1.9–2.0
	λ_{max} in water (nm)	554.0
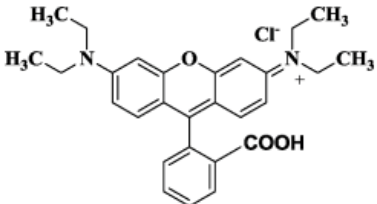
during the study came from Avantor Performance Materials Poland S.A. (Gliwice, Poland).

2.2. Analysis of RhB

The absorbance of rhodamine B was tested using the Jasco V-750 spectrophotometer (Kraków, Poland). Fig. 1 shows the obtained RhB absorption spectrum. The absorption spectrum of the compound shows a peak at the wavelength λ_{max} = 554.0 nm. Model solutions and resulting solutions were tested at this wavelength (λ = 554.0 nm).

2.3. Determination of advanced oxidation parameters

In the first stage of research, the optimal glucose dose was determined. The optimal dose of glucose enables to activate sodium persulfate with visible light. The process was carried out in reaction vessels containing 500.0 cm^{-3} of dye with a concentration of 10.0 mg dm^{-3}. The reaction vessels were placed on a magnetic stirrer for mixing and after stirring the vessels were irradiated with visible light for 60.0 min. The following sugar doses were tested: 100.00; 150.0; 200.0; 300.0 and 500.0 mM. The sodium persulfate dose was 10.0 mM. All experiments were conducted under these conditions: temperature of 295 K, atmospheric pressure equal to 1,013.0 hPa and pH = 6.0.

In order to select the optimal dose of sodium persulfate, the influence of various PDS concentrations was studied. The following doses were tested: 2.0; 5.0; 10.0; 20.0; 50.0 and 100.0 mM. Reaction vessels containing 10.0 mg dm^{-3} dye were placed on a magnetic stirrer.

Optimal process time is a significant parameter from an economic point of view and in terms of total pollutants removal. The study was conducted for 180 min. Samples were collected after 5, 10, 15, 20, 30, 45, 60, 120 and 180 min. Reaction vessels containing the model solution with the addition of a RhB standard at a concentration of 10.0 mg dm^{-3} were placed on a magnetic stirrer to be adequately mixed. The glucose dose was 200.00 mM and the Na$_2$S$_2$O$_8$ dose was 20.0 mM.

The effect of the initial RhB concentration was investigated. Four dye concentrations were used: 1.0, 5.0, 10.0 and 20.0 mg dm^{-3}. Samples were collected after 60.0 min. Reaction

vessels containing the model solution with the addition of tested concentrations were placed on a magnetic stirrer. The glucose dose was 200.00 mM, while the Na$_2$S$_2$O$_8$ dose was 20.0 mM.

All the experiments were carried out independently in triplicate. The data presented in the next section include average values.

2.4. Visible light activated persulfate tests

A 10 W Tungsten QTH10/M lamp from Thorlabs Inc. (New Jersey, United States) was used as the visible radiation source. The lamp emits radiation with a wavelength (λ) from 400 to 2,200 nm. For the purpose of the research, the FGS900M filter (Thorlabs Inc., United States) was used to cut off the spectrum bands above 710 nm. The filter was mounted using a Thorlabs Inc. circular cage system (Thorlabs Inc., United States; Fig. 2). The lamp emitted radiation from the visible light range. The experiments were conducted in an isolated chamber, without the possibility of exposure to another light source.

2.5. Ultrasound activated persulfate tests

Sonication was carried out using a Proclean 0.7 WH ultrasonic generator (Ulsonix Cleaning Instruments, Germany) with a capacity of 0.7 dm^{-3}. Persulfates activation was carried out under the following conditions: output power 60 W, ultrasound frequency 40 kHz, reactor dimensions 150 × 86 × 65 mm.

2.6. Reaction kinetics

According to the scientific literature data [29,30], to describe the decolorization kinetics of most rhodamine dyes, the pseudo-first-order reaction equation can be used (Eq. (2)).

$$-\ln\left(\frac{C}{C_0}\right) = kt \tag{2}$$

where C_0 – concentration of RhB before the purification process (mg dm^{-3}); C – concentration of RhB after the
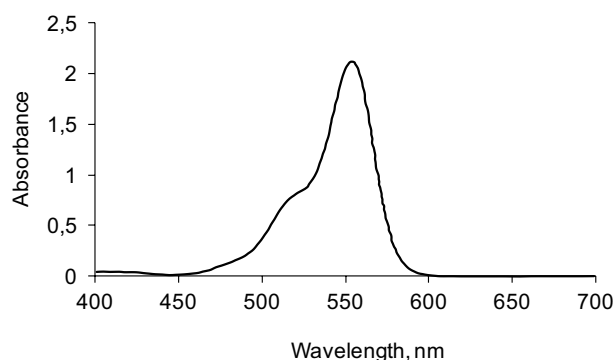
Fig. 1. Absorption spectrum of rhodamine B standard (10.0 mg dm^{-3}).
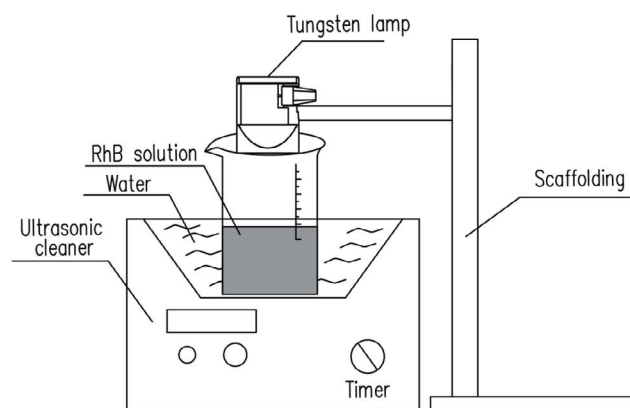
Fig. 2. Illustration of the experimental set-up.

purification process (mg dm^{-3}); k – reaction rate constant; t – reaction time (min).

The half-life of RhB ($t/2$) was calculated mathematically based on the reaction rate constant k as follows:

$$t/2 = \ln(2)/k \qquad (3)$$

2.7. Radical scavenger test

A radical scavenger test was used to determine the major radical types involved in dye degradation. In the study, tert-butyl alcohol (BuOH) was used as an OH$^\bullet$ radical scavenger, methanol (MeOH) as a SO$_4^{\bullet-}$ and OH$^\bullet$ radical scavenger and hydroquinone as an O$_2^{\bullet-}$ radical scavenger. The applied compounds are most commonly used as radical scavengers by many researchers [31–33]. Radical scavengers at a dose of 50.0 μM were added before the AOP.

3. Results and discussion

3.1. Optimal glucose dose

At this stage, the optimal concentration of glucose was determined. The following sugar concentrations were tested: 100.00, 150.0, 200.0, 300.0 and 500.0 mM (Fig. 3). The process was carried out in the presence of visible light for 60 min. The dose of sodium persulfate was 10 mM. In the preliminary tests [20], the decolorization process was carried out in the presence of glucose only, without Na$_2$S$_2$O$_8$ and visible light addition. The results of the study did not confirm the dye degradation in the presence of glucose alone. A concentration of 200.0 mM was selected as the optimal glucose dose for further testing. The decomposition of rhodamine B under these conditions was about 42%. For the other concentrations analysed, the RhB decomposition was unsatisfactory. In addition, a high content of sugar resulted in the reduced effect of decolorization. This is due to the inhibition of radicals by higher glucose levels ($k_{OH^\bullet} = 1.5 \times 10^9$) [34].

Rhodamine B decomposition with addition of glucose may be due to the optical properties of sugar. Glucose is an optically active substance, that is, it tends to rotate the light plane, which may explain the higher dye decomposition in the presence of sugar compared with a solution purified only with persulfate. PDS activation by visible
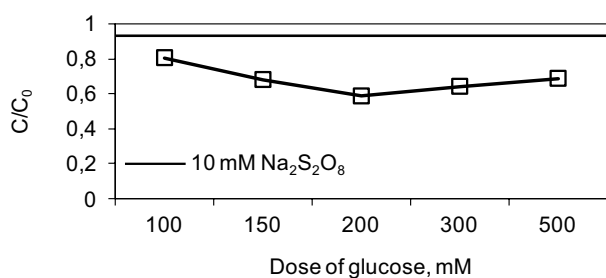
radiation in the presence of glucose may also result from the probable electron transfer from sugar towards PDS and its activation. Moreover glucose oxidation products may be able to activate PDS (Eq. (4)). It is related to the organic PDS activation with an external carbon source [35]. Ahmad et al. [36] performed a research on the activation of persulfates with two organic compounds: phenoxides and phenols. Phenoxides have been proved to be an effective persulfate activator. Literature data show that the mechanism of PDS activation by glucose is similar to the mechanism of activation by phenoxides [23]. Glucose oxidation causes the sugar decomposition, whereby compounds containing a functional group are generated. An example of such functional group is, for example, carbonyl group, which accepts the negative charge activating persulfates.

$$S_2O_8^{2-} + RhB + glucose \xrightarrow{\text{Vis}} e^- + S_2O_8^{2-} +$$
$$RhB \xrightarrow{\text{Vis}} SO_4^{\bullet-} + SO_4^{2-} + \text{by-products}^* \qquad (4)$$
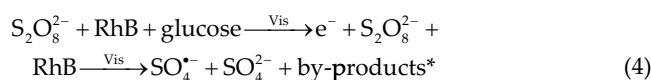
where * indicates that identification of rhodamine B degradation products was beyond the scope of this study.

3.2. Optimal Na$_2$S$_2$O$_8$ dose

The dependence of rhodamine B decolorization on the Na$_2$S$_2$O$_8$ dose is presented in Fig. 4. The process was carried out in the presence of visible light. The following doses of sodium persulfate were tested: 2.0, 5.0, 10.0, 20.0, 50.0 and 100.0 mM. The glucose concentration was 200.0 mM. The process was carried out for 60 min. The RhB decomposition depended on the initial persulfate dose, that is, it increased with increasing PDS dose. The increase in the degree of decolorization results from the increase in the density of generated active species. The addition of 20.0 mM persulfate after 60.0 min caused the dye to be removed in approximately 47%. Higher doses of PDS (50.0 and 100.0 mM) did not cause a significant increase in purification efficiency. Taking into account economic aspects, 20.0 mM was chosen as the optimal dose of Na$_2$S$_2$O$_8$. Degradation of pollutants in the PDS system without the use of catalysts is possible, whereas the degree of removal of organic pollutants without the use of catalysts is lower. Without activation, the persulfate anion will react only with some organic chemicals. The removal degree is smaller than in activated persulfate system, because persulfate

Fig. 3. Influence of glucose dose on the rhodamine B decolorization. Conditions: $C_{0[RhB]}$ = 10.0 mg dm^{-3}; pH = 6.0; reaction time = 60.0 min; Na$_2$S$_2$O$_8$ dose = 10.0 mM.
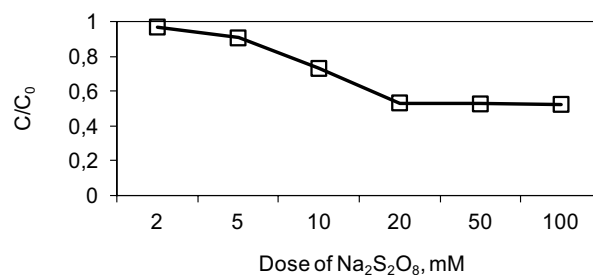
Fig. 4. Influence of the Na$_2$S$_2$O$_8$ dose on the rhodamine B decolorization. Conditions: $C_{0[RhB]}$ = 10.0 mg dm^{-3}; pH = 6.0; reaction time = 60.0 min; glucose concentration = 200.0 mM.

ion (E^0 = 2.01 V) has lower oxidation potential compared with sulfate ion (E^0 = 2.50–3.10 V) [37].

3.3. Optimal RhB decomposition time

Fig. 5a depicts the influence of process time on the degree of RhB decolorization in $Na_2S_2O_8$, US, $Na_2S_2O_8$/Vis and $Na_2S_2O_8$/US systems. Process was carried out for 180.0 min. It was found that the dye decolorization effect increased with the duration time. After 30 min of the process, the efficiency of the $Na_2S_2O_8$/Vis system was 32%, while in the $Na_2S_2O_8$/US system it was 49%. A satisfying decolorization effect was achieved after 60.0 min of reaction. In that time, the dye decomposition was 49% and 67% for visible and ultrasound activated persulfate, respectively. As shown in Fig. 5, continuation of the process caused a slight increase in efficiency by about 1%–2%. Ultrasound (US) cleaning had the least effect on the decomposition of rhodamine B. The decomposition of this compound did not exceed 25% after 180.0 min. The highest degree of dye removal was obtained in the combined visible–ultrasound system ($Na_2S_2O_8$/Vis/US). About 85% RhB was removed within 60.0 min in this system, whereas after 180.0 min the degradation efficiency slightly increased to 95.0%. Due to the need to limit reactor volume during plant design and a slight difference in the decomposition degree after 120.0 and 180.0 min of the purification process, 60.0 min time of reaction was selected as the optimal contact time.

Persulfate activation in the $Na_2S_2O_8$/Vis system is the result of a synergistic relationship between visible light and the enhanced effect of glucose electron transfer from this sugar towards persulfate (Eq. (5)). The study by Zawadzki [20] showed that the addition of only sugar without visible light irradiation does not contribute to the activation of persulfate. Scientific literature data indicates that in an alkaline reaction (pH = 6.0), in which the present experiments were carried out, the addition of glucose promotes persulfate activation since its functional groups (e.g., carbonyl group) accept partially negative charge.

$$S_2O_8^{2-} + RhB + glucose \xrightarrow{\text{Vis}} e^- + S_2O_8^{2-} +$$
$$RhB \xrightarrow{\text{Vis}} SO_4^{\bullet-} + SO_4^{2-} \tag{5}$$
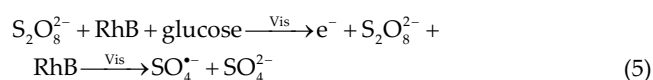
As shown in Fig. 5a, it was established that the decolorization effect in the $Na_2S_2O_8$/US system was higher compared with the $Na_2S_2O_8$/Vis system. First of all, this is because of the applied persulfate activation method.

In the ultrasound activated persulfates, the role of ultrasound occurs in two possible ways [38,39]. In the first mechanism, persulfate is activated by heat from ultrasonic cavitation (Eq. (6)), which generates cavitation bubbles. During the ultrasound process, the cavitation bubbles break down, which locally causes the formation of high temperatures ($T \approx 5,000$ K) and pressure ($P \approx 1,000$ atm). As reported by Fedorov et al. [40], equally to conventional persulfate activation methods, the energy released during the collapse of the cavitation bubbles catalyse the activation of persulfate to produce $SO_4^{\bullet-}$ radicals. Ultrasound cleaning can induce a cavitation phenomenon, which is an essential agent in the activation of persulfates. A study by Ghanbari and Moradi [41] showed that this process is found to consist of numerous reverse and side reactions generating $SO_4^{\bullet-}$ and $OH^\bullet$ radicals.

In the second mechanism, cavitation bubbles initiate the dissociation of water molecules to generate hydroxyl radical (Eq. (7)). Dissociation of water molecules takes place inside the bubbles as well as in the interface between the gas phase and surrounding liquid [42]. Generated hydroxyl radical attacks persulfate ions forming sulfate radical anion ($SO_4^{\bullet-}$), bisulfate ion and oxygen (Eqs. (8) and (9)).

$$S_2O_8^{2-} \xrightarrow{\text{heat}} 2SO_4^{\bullet-} \tag{6}$$

$$H_2O \xrightarrow{\text{)))}} OH^\bullet + H^\bullet \tag{7}$$

where the symbol ")))" indicates ultrasound.

$$S_2O_8^{2-} + OH^\bullet \rightarrow H^+ + SO_4^{2-} + SO_4^{\bullet-} + \frac{1}{2}O_2 \tag{8}$$

$$SO_4^{\bullet-} + H_2O \rightarrow OH^\bullet + HSO_4^{2-} \tag{9}$$
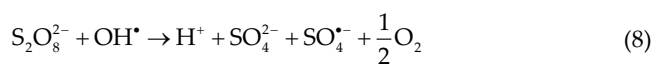
Conducted studies confirm that the Langmuir–Hinshelwood (L-H) model can be used to describe the kinetics of rhodamine B degradation. This result can be justified by considering Fig. 5b. The analysis of the correlation coefficient R^2 showed very good fit of experimental data (95%–99%). Half-life $t/2$ and reaction rate constants k were determined using the L-H model. The results are summarized in Table 2. Taking into account the relationship
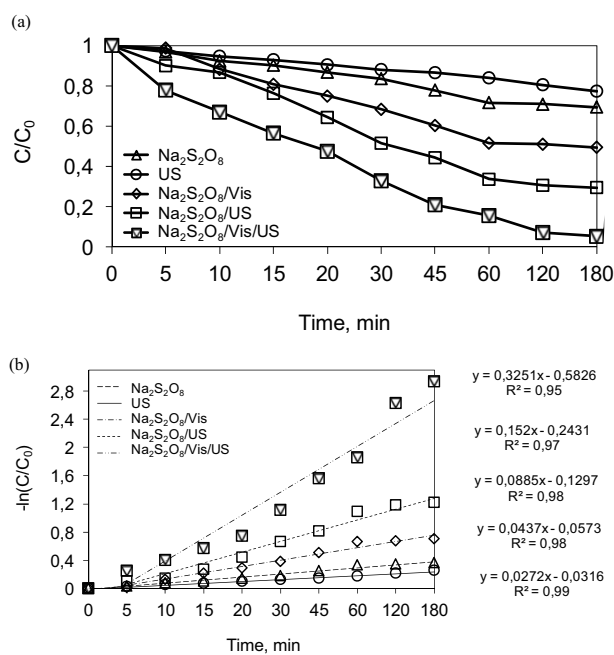
Fig. 5. Influence of reaction time on the rhodamine B decomposition in various systems (a) and reaction kinetics (b). Conditions: $C_{0[RhB]}$ = 10 mg dm^{-3}; glucose dose = 200.0 mM; $Na_2S_2O_8$ dose = 20.0 mM; pH = 6.0; US frequency = 40.0 kHz; temperature = 295 K; US power = 60 W.

Table 2
Parameters of pseudo-first-order reaction

Process	k (min^{-1})	R^2	$t/2$ (min)
Na$_2$S$_2$O$_8$	0.044	0.98	15.9
US	0.027	0.99	25.5
Na$_2$S$_2$O$_8$/Vis	0.089	0.98	7.8
Na$_2$S$_2$O$_8$/US	0.152	0.97	4.6
Na$_2$S$_2$O$_8$/Vis/US	0.325	0.95	2.1

Table 3
Classification of reaction rate based on half-life [46]

Half-life, s	Time span for near-completion	Rate classification
10^{-15}–10^{-12}	ps or less	Ultra fast rate
10^{-12}–10^{-6}	μs or less	Very fast rate
10^{-6}–1	Seconds	Fast rate
1–10^3	minutes or hours	Moderate rate
10^6–10^3	Weeks	Slow rate
>10^6	weeks or years	Very slow rate

between $-\ln(C/C_0)$ and reaction time, the two-stage oxidation process, which is a characteristic phenomenon, for example, for heterogeneous oxidation processes [43,44] was not found. The two-stage oxidation process is mainly attributed to the indirect reaction of oxygenating species with by-products or decreasing amount of radicals during the reaction. However, the identification of intermediates was beyond the scope of this study.

The results indicate that the activation of persulfate affects the kinetic parameters of rhodamine B degradation. Reaction rate constant k was the lowest in the case of the ultrasonic cleaning process. As reported in the study by Hou et al. [45], this is due to the small amount of radicals generated during the fragmentation of water molecules. The highest value of the reaction rate constant was observed in the combined system (Na$_2$S$_2$O$_8$/Vis/US). The mathematically calculated half-life ($t/2$) of RhB in this system was 2.1 min.

Table 3 presents the classification of the chemical reaction rate based on the mathematically calculated half-life $t/2$. The dynamics of ultrasonic cleaning was the lowest among the processes tested. The reaction was classified as slow. Four out of five treatment systems tested were found to be at a moderate rate (<10^3 s).

3.4. Effects of different RhB concentrations

The efficiency of rhodamine B decolorization has been studied depending on different dye concentrations (1, 5, 10 and 20 mg dm^{-3}). The process was carried out for 60 min. Abatement curves are shown in Fig. 6. It was found that the final dye concentration depends on its initial concentration. This is common for both AOPs [47] and activated persulfates [48]. Because the conditions for each of the experiments were the same (Na$_2$S$_2$O$_8$, dose, glucose dose, pH, temperature), the amount of sulfate radicals generated was constant and decreased with increasing RhB concentration. As shown in the study by Cai et al. [49], the collision probability of oxygenating radicals decreases with increasing concentration of dye molecules. High concentration of dye molecules causes greater consumption of radicals resulting in an insufficient amount of radicals to decompose the excess of RhB. This results in a reduced efficiency of dye removal. Moreover, intermediates may consume active species, which results in a poor dye decolorization (competitiveness effect). Despite the unfavorable conditions for RhB degradation (high dye concentration), the combination of visible light and ultrasound persulfate activation

Fig. 6. Efficiency of rhodamine B decolorization depending on the initial dye concentration in various systems. Conditions: reaction time = 60.0 min; pH = 6.0; US frequency = 40.0 kHz; US power = 60 W; temperature = 295 K; Na$_2$S$_2$O$_8$ dose = 20.0 mM; glucose dose = 200.0 mM.

processes (Na$_2$S$_2$O$_8$/Vis/US) allowed to achieve a high RhB degradation at the level of 80% at the highest dye concentration (20.0 mg dm^{-3}). In comparison, similar efficiency was obtained in the Na$_2$S$_2$O$_8$/US system, but at the lowest concentration (1.0 mg dm^{-3}).

When only ultrasound is used, a similar situation can be observed. With an increasing RhB concentration, a decrease in the efficiency of rhodamine B decomposition was noticed. Similar to the Na$_2$S$_2$O$_8$, Na$_2$S$_2$O$_8$/Vis and Na$_2$S$_2$O$_8$/US systems, this is due to the amount of radicals generated. The amount of radicals generated in high dye concentrations is insufficient to break down excess of RhB particles. As the literature data shows, the other reason is the changing viscosity of the solution at high dye concentrations. It creates a barrier to the enucleation process, thus insufficient amount of radicals is formed [50].

3.5. Radical scavenger tests

Identification of the main active species was carried out for the combined Na$_2$S$_2$O$_8$/Vis/US process. It was the most effective of all the tested systems; therefore it was selected for further studies. Radical scavengers were used at a concentration of 50.0 mM. The process was carried out for 60 min. Radical scavenger test has been carried out with and without SO$_4^{\bullet-}$, OH$^\bullet$ and O$_2^{\bullet-}$ scavengers to evaluate their influence on RhB degradation. The resulting solution without the addition of scavengers was marked as "control". RhB degradation is essentially inhibited by all scavengers

presented in the solution. This indicates that sulfate $SO_4^{•-}$, hydroxyl $OH^•$ and superoxide $O_2^{•-}$ radicals are generated. As shown in Fig. 8a, the addition of BuOH and MeOH most inhibited the decomposition of rhodamine B. This indicates the significant role of sulfate and hydroxyl radicals in the dye degradation reaction carried out in the presence of persulfate activated with visible light and ultrasound. The addition of hydroquinone ($k_{O_2^{•-}} = 1.7 \times 10^7$ M^{-1} s^{-1}) [51] did not significantly affect the degradation process in its initial phases. Within 5–20 min, the inhibition of RhB degradation efficiency is insignificant. Inhibition becomes visible after 20 min, which may indicate delayed formation of $O_2^{•-}$ radicals.

The obtained results were similar to those obtained by Nasseri et al. [11], who applied a radical scavenger test on peroxydisulfate activated by ultrasound irradiation. It was concluded that $OH^•$ radical was found to be predominant for the degradation by US/PDS process.

The results showed that under following conditions: RhB concentration = 10.0 mg dm^{-3}; Na$_2$S$_2$O$_8$ dose = 20.0 mM; pH = 6.0; T = 295 K; glucose dose = 200.0 mM; US frequency = 40.0 kHz; US power = 60 W, RhB degradation was inhibited by nearly 80% by methanol addition. Methanol is a strong scavenger for hydroxyl and weaker for sulfate radicals, while tert-butyl alcohol inhibits only sulfate radicals (Eqs. (10)–(13)) [52].

$$BuOH + OH^• \sim 5.2 \times 10^8 \, M^{-1} s^{-1} \tag{10}$$

$$BuOH + SO_4^{•-} \sim \leq 10^6 \, M^{-1} s^{-1} \tag{11}$$

$$MeOH + OH^• \sim 8.0 \times 10^8 \, M^{-1} s^{-1} \tag{12}$$

$$MeOH + SO_4^{•-} \sim 1.0 \times 10^7 \, M^{-1} s^{-1} \tag{13}$$
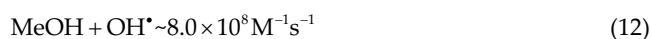
The Na$_2$S$_2$O$_8$/Vis/US process has shown promising efficiency in the degradation of rhodamine B. The degradation degree was significantly inhibited by the addition of methanol (MeOH) and tert-butyl alcohol (BuOH). The results indicate that the RhB degradation was primarily due to hydroxyl radicals, and second due to sulfate radicals. Therefore, the degradation of RhB is attributed to $OH^•$ radical. Literature data reported that the hydroxyl radical is formed in the reaction of $SO_4^{•-}$ with water at the whole range of pH values [53]. Hence, degradation of RhB can be explained by the radical mechanism. Those results are corresponding with the data reported by Lu et al. [54].

To study in detail the mechanism of RhB degradation, not only the absorbance value at the wavelength λ_{max} = 554.0 nm was considered but also a full UV-Vis spectrum (λ = 200–800 nm) of the rhodamine B resulting solutions treated in the Na$_2$S$_2$O$_8$/Vis/US process was taken into account, as presented in Fig. 7. Two phenomena were observed during the Na$_2$S$_2$O$_2$/Vis/US experiment. First, which was also reported by Wang et al. [55], the absorbance intensity decreased with the process time, as observed in section 3.3. Then, maximum absorbance shift (around 3 nm) was found after 45 min of decolorization (λ_{max} = 551 nm).

After 60 min of the process, the shift of the absorption peak was set to approximately 6 nm (λ_{max} = 548 nm). In literature, this phenomenon is found as a hypsochromic shift. In the first case, the reduction of RhB concentration is attributed to chromophore cleavage. Bleaching through the cleavage of conjugated chromophore structure is one of the possible mechanisms of RhB degradation in the AOPs such as photocatalysis and persulfate oxidation [56]. Literature [57,58] revealed that for photodegradation process under visible light irradiation, for some of N-alkylamine-containing dyes (e.g., crystal violet or rhodamine B), the absorption shift is related to the N-demethylation. However, since the absorption shift is insignificant, the major mechanism of rhodamine B degradation in the Na$_2$S$_2$O$_8$/Vis/US process is the process of N-deethylation.

The study of reaction kinetics confirmed the above observations. The values of pseudo-first-order reaction and their regression coefficients R^2 are presented in Table 4. Based on experimental results, kinetics of RhB decolorization showed a significant difference in the rate of dye degradation after the addition of radical scavengers. A logarithmic trendline has been shown in Fig. 8b. As a result of the inhibition of hydroxyl and sulfate radicals, the mathematically calculated half-life increased from 2.7 to 10.6 min and then to 24.7 min after the addition of BuOH and MeOH, respectively. The reaction between hydroquinone and $O_2^{•-}$ radicals resulted in a 46% increase in half-life comparing with the control sample. The reaction rate constant was the lowest after the addition of methanol. These findings are similar to previous studies in the persulfate oxidation system [59].

4. Comparison with other AOPs systems

As presented in Table 5, the proposed method is an interesting alternative to eliminate RhB in comparison with prior studies conducted by the researchers. As is shown, the Na$_2$S$_2$O$_8$/Vis/US process has great potential for the degradation of rhodamine B, particularly where the dye concentrations are not high (up to 20 mg dm^{-3}). Energy-saving equipment, relatively short reaction time (60.0 min) and low consumption of reagents are benefits of using this method.
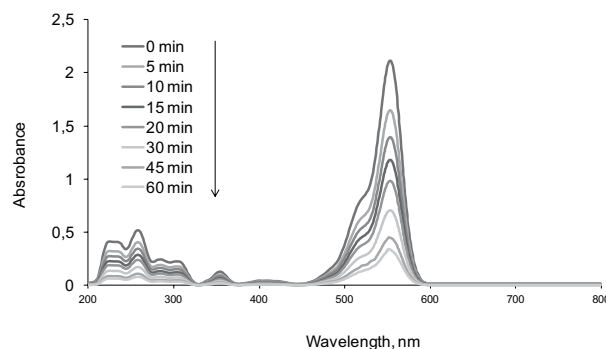
Fig. 7. UV-vis absorption spectra of RhB model solution. Conditions: $C_{0[RhB]}$ = 10.0 mg dm^{-3}; Na$_2$S$_2$O$_8$ dose = 20.0 mM; pH = 6.0; T = 295 K; glucose dose = 200.0 mM; US frequency = 40.0 kHz; US power = 60 W.

Table 4
Parameters of pseudo-first-order reaction

Process	k (1/min)	R^2	$t/2$ (min)
$Na_2S_2O_8$/Vis/US (control)	0.2601	0.96	2.7
$Na_2S_2O_8$/Vis/US + MeOH	0.0281	0.83	24.7
$Na_2S_2O_8$/Vis/US + BuOH	0.0655	0.93	10.6
$Na_2S_2O_8$/Vis/US + hydroquinone	0.1396	0.98	5.0

The proposed method is characterized by a low-power radiation source (10 W compared with e.g., 300 W in the study by Wang et al. [60]). The reaction time needed to achieve 85% decolorization is over five times shorter compared with the research performed by Zhang et al. [61]. To limit residual reagents and harmful by-products in the AOP effluent, process optimization should be carried out for specific wastewater.

5. Conclusions

This study showed that the activation of sodium persulfate in the combined visible light–ultrasound system significantly affects the degree of rhodamine B decolorization. Sodium persulfate activated by visible light and ultrasound proved to be highly efficient in the decomposition of rhodamine B. In this system, the degree of rhodamine B decolorization after 60.0 min of reaction was 85%. After 60.0 min of the reaction, mathematically calculated half-life in the $Na_2S_2O_8$/Vis/US system was only 2.1 min under the following conditions: $Na_2S_2O_8$ dose of 20.0 mM; glucose dose of 200.0 mM; US power = 60 W; US frequency = 40 kHz; RhB concentration of 10.0 mg dm^{-3} and initial pH at 6.0. For this system, half-life was over seven times higher compared with the purification process carried out in the presence of $Na_2S_2O_8$ only. Activation of sodium persulfate in the combined system showed high resistance to high RhB concentrations. An 80% of the dye was decomposed after 60.0 min reaction at a concentration of 20.0 mg dm^{-3} in contrast to 40% in a system purified only with persulfate at a concentration of 1.0 mg dm^{-3}. It was determined
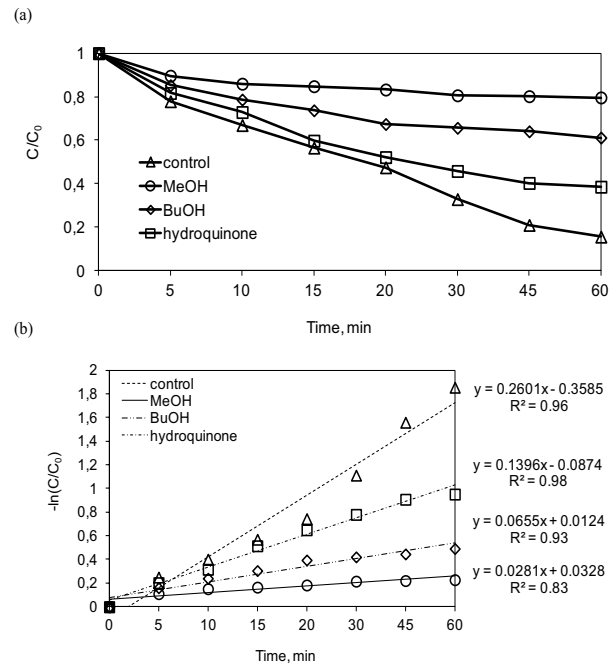
Fig. 8. Decomposition of rhodamine B in the presence of various radical scavengers (a) and reaction kinetics (b). Conditions: $C_{0[RhB]}$ = 10.0 mg dm^{-3}; $Na_2S_2O_8$ dose = 20.0 mM; pH = 6.0; T = 295 K; glucose dose = 200.0 mM; US frequency = 40.0 kHz; US power = 60 W.

that sulfate and hydroxyl radicals were mainly responsible for the decolorization of rhodamine B. Hydroxyl radicals were the dominant radicals enabling RhB degradation.

Funding

Table 5
Efficiency of Rhodamine B degradation in different AOPs

Process	Conditions	Efficiency (%)	Literature
$Na_2S_2O_8$/Vis/US	Reaction time = 60.0 min; $C_{0[RhB]}$ = 10.0 mg dm^{-3}; $Na_2S_2O_8$ dose = 20.0 mM; pH = 6.0; T = 295 K; glucose dose = 200.0 mM; lamp = 10 W; US frequency = 40.0 kHz; US power = 60 W	85.0	This study
Feather keratin/ CdS/Vis	Reaction time = 70.0 min; $C_{0[RhB]}$ = 20.0 mg dm^{-3}; FK/CdS dose = 10 g dm^{-3}; lamp = 300 W	96.6	[60]
Au-ZnO/Vis	Reaction time = 330.0 min; $C_{0[RhB]}$ = 1.0 mg dm^{-3}; Au-ZnO dose = 500 mg dm^{-3}; pH = 4.76; lamp = 300 W	92.0	[61]
Electro-Fenton	Reaction time = 180.0 min; $C_{0[RhB]}$ = 10 mg dm^{-3}; electrode dose = 15 mg dm^{-3}; pH = 2.0; voltage = 8 V	97.7	[62]
Carbon aerogel/ persulfate	Reaction time = 60.0 min; $C_{0[RhB]}$ = 10 mg dm^{-3}; persulfate dose = 1.0 mM; pH = 7.0; T = 298 K; carbon aerogel dose = 100 mg dm^{-3}	80.0	[63]

References

[1] Global Water Crisis, The Facts, 2020. Available at: https://inweh.unu.edu/wp-content/uploads/2017/11/Global-Water-Crisis-The-Facts.pdf (Accessed on: 10 May 2020).

[2] R. Tröger, P. Klöckner, L. Ahrens, K. Wiberg, Micropollutants in drinking water from source to tap - method development and application of a multiresidue screening method, Sci. Total Environ., 627 (2018) 1404–1432.

[3] C.C. Montagner, F.F. Sodré, R.D. Acayaba, C. Vidal, I. Campestrini, M.A. Locatelli, I.C. Pescara, A.F. Albuquerque, G.A. Umbuzeiro, W.F. Jardim, Ten years-snapshot of the occurrence of emerging contaminants in drinking, surface and ground waters and wastewaters from São Paulo State, Brazil, J. Braz. Chem. Soc., 30 (2019) 614–632.

[4] J. Kozak, M. Włodarczyk-Makuła, Comparison of the PAHs degradation effectiveness using CaO_2 or H_2O_2 under the photo-Fenton reaction, Desal. Water Treat., 134 (2018) 57–64.

[5] J. Kozak, M. Włodarczyk-Maukła, The use of sodium percarbonate in the Fenton reaction for the PAHs oxidation, Civil Environ. Eng. Rep., 28 (2018) 124–139.

[6] K. Shakir, A.F. Elkafrawy, H.F. Ghoneimy, S.G. Elrab Beheir, M. Refaat, Removal of rhodamine B (a basic dye) and thoron (an acidic dye) from dilute aqueous solutions and wastewater simulants by ion flotation, Water Res., 44 (2010) 1449–1461.

[7] L. Yu, Y. Mao, L. Qu, Simple voltammetric determination of Rhodamine B by using the glassy carbon electrode in fruit juice and preserved fruit, Food Anal. Methods, 6 (2013) 1665–1670.

[8] S.S. Imam, H.F. Babamale, A short review on the removal of rhodamine B dye Rusing agricultural waste-based adsorbents, Asian J. Chem. Sci., 7 (2020) 25–37.

[9] B. Dogan, M. Kerestecioglu, U. Ulku Yetis, Assessment of the best available wastewater management techniques for a textile mill: cost and benefit analysis, Water Sci. Technol., 61 (2010) 963–970.

[10] R. Zhang, P. Sun, T.H. Boyer, L. Zhao, C.H. Huang, Degradation of pharmaceuticals and metabolite in synthetic human urine by UV, UV/H_2O_2, and UV/PDS, Environ. Sci. Technol., 49 (2015) 3056–3066.

[11] S. Nasseri, A.H. Mahvi, M. Seyedsalehi, K. Yaghmaeian, R. Nabizadeh, M. Aliomohammadi, G.H. Safari, Degradation kinetics of tetracycline in aqueous solutions using peroxydisulfate activated by ultrasound irradiation: effect of radical scavenger and water matrix, J. Mol. Liq., 241 (2017) 704–714.

[12] S.A. Hakim, S. Jaber, N.Z. Eddine, A. Baalbaki, A. Ghauch, Data for persulfate activation by UV light to degrade theophylline in a water effluent, Data Brief, 27 (2019) 104614.

[13] Y. Ji, W. Xie, Y. Fan, Y. Shi, D. Kong, J. Lu, Degradation of trimethoprim by thermo-activated persulfate oxidation: reaction kinetics and transformation mechanisms, Chem. Eng. J., 286 (2016) 16–24.

[14] J. Criquet, N.K. Vel Leitner, Electron beam irradiation of aqueous solution of persulfate ions, Chem. Eng. J., 169 (2011) 258–262.

[15] O. Furman, A.L. Teel, R.J. Watts, Mechanism of base activation of persulfate, Environ. Sci. Technol., 44 (2010) 6423–6428.

[16] M. Nie, C. Yan, M. Li, X. Wang, W. Bi, W. Dong, Degradation of chloramphenicol by persulfate activated by Fe^{2+} and zerovalent iron, Chem. Eng. J., 279 (2015) 507–515.

[17] G.P. Anipsitakis, D.D. Dionysiou, Radical generation by the interaction of transition metals with common oxidants, Environ. Sci. Technol., 38 (2004) 3705–3712.

[18] W.S. Chen, Y.C. Su, Removal of dinitrotoluenes in wastewater by sono-activated persulfate, Ultrason. Sonochem., 19 (2012) 921–927.

[19] X. Cheng, H. Guo, Y. Zhang, G. Korshin, B. Yang, Insights into the mechanism of nonradical reactions of persulfate activated by carbon nanotubes: activation performance and structure-function relationship, Water Res., 157 (2019) 406–414.

[20] P. Zawadzki, Decolorisation of Methylene Blue with sodium persulfate activated with visible light in the presence of glucose and sucrose, Water Air Soil Pollut., 230 (2019) 1–18.

[21] W. Wang, H. Wang, G. Li, T. An, H. Zhao, P.K. Wong, Catalyst-free activation of persulfate by visible light for water disinfection: efficiency and mechanisms, Water Res., 157 (2019) 106–118.

[22] H. Herrmann, On the photolysis of simple anions and neutral molecules as sources of O^-/OH, SO_{x^-} and Cl in aqueous solution, Phys. Chem. Chem. Phys., 9 (2007) 3935–3964.

[23] R.J. Watts, M. Ahmad, A.K. Hohner, A.L. Teel, Persulfate activation by glucose for in situ chemical oxidation, Water Res., 133 (2018) 247–254.

[24] P. Gayathri, R.P.J. Dorathi, K. Palanivelu, Sonochemical degradation of textile dyes in aqueous solution using sulphate radicals activated by immobilized cobalt ions, Ultrason. Sonochem., 17 (2010) 566–571.

[25] G.J. Price, A.A. Clifton, Sonochemical acceleration of persulfate decomposition, Polymer, 37 (1996) 3971–3973.

[26] K.H. Chu, Y.A.J. Al-Hamadani, C.M. Park, G. Lee, M. Jang, A. Jang, N. Her, A. Son, Y. Yoon, Ultrasonic treatment of endocrine disrupting compounds, pharmaceuticals, and personal care products in water: a review, Chem. Eng. J., 327 (2017) 629–647.

[27] A.B. Kurukutla, P.S.S. Kumar, S. Anandan, T. Sivasankar, Sonochemical degradation of Rhodamine B using oxidants, hydrogen peroxide/peroxydisulfate/peroxymonosulfate, with Fe^{2+} ion: proposed pathway and kinetics, Environ. Eng. Sci., 32 (2015) 129–140.

[28] Rhodamine B. Available at: https://pubchem.ncbi.nlm.nih.gov/compound/Rhodamine-B, 2020 (Accessed on: 10 May 2020).

[29] K.P. Wai, Y.L. Pang, S. Lim, C.H. Koo, W.C. Chong, Hydrothermal modification of zinc oxide and titanium dioxide for photocatalytic degradation of Rhodamine B, AIP Conf. Proc., 2157 (2019) 020006.

[30] D. Melgoza, A. Hernandez-Ramirez, J.M. Peralta-Hernandez, Comparative efficiencies of the decolourisation of methylene blue Rusing Fenton's and photo-Fenton's reactions, Photochem. Photobiol. Sci., 8 (2009) 596–599.

[31] D. Nakarada, M. Petkovic, Mechanistic insights on how hydroquinone disarms OH and OOH radicals, Quantum Chem., 118 (2018) 1–14.

[32] J. Wang, S. Wang, Activation of persulfate (PS) and peroxymonosulfate (PMS) and application for the degradation of emerging contaminants, Chem. Eng. J., 334 (2018) 1502–1517.

[33] H. Azarpira, M. Sadani, M. Abtahi, N. Vaezi, S. Rezaei, Z. Atafar, S.M. Mohseni, M. Sarkhosh, M. Ghaderpoori, H. Keramati, R.H. Pouyaj, A. Akbari, V. Fanai, Photo-catalytic degradation of triclosan with UV/iodide/ZnO process: performance, kinetic, degradation pathway, energy consumption and toxicology, J. Photochem. Photobiol. A, 371 (2019) 423–432.

[34] G.V. Buxton, C.L. Greenstock, W.P. Helman, A.B. Ross, Critical review of rate constants for reactions of hydrated electrons, hydrogen atoms and hydroxyl radicals ($^\bullet OH/^\bullet O^-$) in aqueous solution, J. Phys. Chem. Ref. Data, 17 (1988) 513–886.

[35] T. Cai, Y. Liu, L. Wang, W. Dong, H. Chen, W. Zeng, X. Xia, G. Zeng, Activation of persulfate by photoexcited dye for antibiotic degradation: radical and nonradical reactions, Chem. Eng. J., 375 (2019) 122070.

[36] M. Ahmad, A.L. Teel, R.J. Watts, Mechanism of persulfate activation by phenols, Environ. Sci. Technol., 47 (2013) 5864–5871.

[37] S. Ahmadi, Ch.A. Igwegbe, S. Rahdar, The application of thermally activated persulfate for degradation of Acid Blue 92 in aqueous solution, Int. J. Ind. Chem., 10 (2019) 1–12.

[38] Z. Wei, F.A. Villamena, L.K. Weavers, Kinetics and mechanism of ultrasonic activation of persulfate: an in-situ EPR spin trapping study, Environ. Sci. Technol., 51 (2017) 3410–3417.

[39] J.M. Monteagudo, A. Duran, R. Gonzalez, A.J. Exposito, In situ chemical oxidation of carbamazepine solutions using persulfate simultaneously activated by heat energy, UV light, Fe^{2+} ions, and H_2O_2, Appl. Catal., B, 176–177 (2015) 120–129.

[40] K. Fedorov, M. Plata-Gryl, J.A. Khan, G. Boczkaj, Ultrasound-assisted heterogeneous activation of persulfate and peroxymonosulfate by asphaltenes for the degradation of BTEX in water, J. Hazard. Mater., 397 (2020) 122804.

[41] F. Ghanbari, M. Moradi, Application of peroxymonosulfate and its activation methods for degradation of environmental organic pollutants: review, Chem. Eng. J., 310 (2017) 41–62.

[42] C.H. Weng, K.L. Tsai, Ultrasound and heat enhanced persulfate oxidation activated with Fe^0 aggregate for the decolorization of C.I. Direct Red 23, Ultrason. Sonochem., 29 (2016) 11–18.

[43] P. Zawadzki, E. Kudlek, M. Dudziak, Kinetics of the photocatalytic decomposition of bisphenol A on modified photocatalysts, J. Ecol. Eng., 19 (2018) 260–268.

[44] E. Kudlek, M. Dudziak, G. Kamińska, J. Bohdziewicz, Kinetics of the photocatalytic degradation of selected organic micropollutants in the water environment, J. Ecol. Eng., 18 (2017) 75–82.

[45] L.W. Hou, H. Zhang, L.G. Wang, L. Chen, Y.D. Xiong, X.F. Xue, Removal of sulfamethoxazole from aqueous solution by sono-ozonation in the presence of a magnetic catalyst, Sep. Purif. Technol., 117 (2013) 46–52.

[46] M.R. Wright, An Introduction to Chemical Kinetics, John Wiley and Sons, England, 2004.

[47] J.P. Zotesso, E.S. Cossich, V. Janeiro, C.R.G. Tavares, Treatment of hospital laundry wastewater by UV/H_2O_2 process, Environ. Sci. Pollut. Res., 24 (2017) 6278–6287.

[48] F. Liu, P. Yi, X. Wang, H. Gao, H. Zhang, Degradation of Acid Orange 7 by an ultrasound/ZnO-GAC/persulfate process, Sep. Purif. Technol., 194 (2018) 181–187.

[49] C. Cai, H. Zhang, X. Zhong, L.W. Hou, Ultrasound enhanced heterogeneous activation of peroxymonosulfate by a bimetallic Fe-Co/SBA-15 catalyst for the degradation of Orange II in water, J. Hazard. Mater., 283 (2015) 70–79.

[50] K. Thangavadivel, M. Megharaj, A. Mudhoo, R. Naidu, Degradation of Organic Pollutants Using Ultrasound, S.K. Sharma, A. Mudhoo, Eds., Handbook on Application of Ultrasound: Sonochemistry for Sustainability, CRC Press, Taylor & Francis Group, 2011, pp. 447–474.

[51] P.S. Rao, E. Hayon, Redox potentials of free radicals. IV. Superoxide and hydroperoxy radicals $^\bullet O_2^-$ and $^\bullet HO_2$, J. Phys. Chem., 79 (1975) 397–402.

[52] A.M. Ocampo, Persulfate Activation by Organic Compounds, Washington State University, Washington, 2009, pp. 1–77.

[53] J.Y. Zhao, Y. Zhang, X. Quan, S. Chen, Enhanced oxidation of 4-chlorophenol using sulfate radicals generated from zero-valent iron and peroxydisulfate at ambient temperature, Sep. Purif. Technol., 71 (2010) 302–307.

[54] Y. Lu, X. Yang, L. Xu, Z. Wang, Y. X., G. Qian, Sulfate radicals from Fe^{3+}/persulfate system for Rhodamine B degradation, Desal. Water Treat., 57 (2016) 1–10.

[55] S. Wang, Y. Jia, L. Song, H. Zhang, Decolorization and mineralization of Rhodamine B in aqueous solution with a triple system of Cerium(IV)/H_2O_2/hydroxylamine, ACS Omega, 3 (2018) 18456–18465.

[56] Y. Fan, G. Chen, D. Li, Y. Luo, N. Lock, A.P. Jensen, A. Mamakhel, J. Mi, S.B. Iversen, Q. Meng, B.B. Iversen, Highly selective Deethylation of Rhodamine B on TiO_2 prepared in supercritical fluids, Int. J. Photoenergy, 173865 (2012) 1–7.

[57] X. Hu, T. Moohamood, W. Ma, C. Chen, J. Zhao, Oxidative decomposition of Rhodamine B dye in the presence of VO_2^+ and/or Pt(IV) under Visible Light Irradiation: N-Deethylation, chromophore cleavage, and mineralization, J. Phys. Chem. B, 110 (2006) 26012–26018.

[58] C. Lops, A. Ancona, K. Di Cesare, B. Dumontel, N. Garino, G. Canavese, S. Hernandez, V. Cauda, Sonophotocatalytic degradation mechanisms of Rhodamine B dye via radicals generation by micro- and nano-particles of ZnO, Appl. Catal. B Environ., 243 (2019) 629–640.

[59] H. Wang, W. Guo, R. Yin, J. Du, Q. Wu, H. Luo, B. Liu, F. Sseguya, N. Ren, Biochar-induced Fe(III) reduction for persulfate activation in sulfamethoxazole degradation: insight into the electron transfer, radical oxidation and degradation pathways, Chem. Eng. J., 362 (2019) 561–569.

[60] Q. Wang, J. Lian, Q. Ma, Y. Bai, J. Tong, J. Zhong, R. Wang, H. Huang, B. Su, Photodegradation of Rhodamine B over a novel photocatalyst of feather keratin decorated CdS under visible light irradiation, New J. Chem., 9 (2015) 7112–7119.

[61] Y. Zhang, J. Zhou, Z. Li, Q. Feng, Photodegradation pathway of rhodamine B with novel Au nanorods @ ZnO microspheres driven by visible light irradiation, J. Mater. Sci., 53 (2018) 3149–3162.

[62] R. Jinisha, R. Gandhimathi, S.T. Ramesh, P.V. Nidheesh, S. Velmathi, Removal of rhodamine B dye from aqueous solution by electro-Fenton process using iron-doped mesoporous silica as a heterogeneous catalyst, Chemosphere, 200 (2018) 446–454.

[63] L. Jiang, Y. Zhang, M. Zhou, L. Liang, K. Li, Oxidation of Rhodamine B by persulfate activated with porous carbon aerogel through a non-radical mechanism, J. Hazard. Mater., 358 (2018) 53–61.